Hindawi Publishing Corporation
Advances in Meteorology
Volume 2015, Article ID 959284, 18 pages
http://dx.doi.org/10.1155/2015/959284

Research Article

Tropospheric NO_2 Trends over South Asia during the Last Decade (2004–2014) Using OMI Data

Zia ul-Haq, Salman Tariq, and Muhammad Ali

Remote Sensing and GIS Group, Department of Space Science, University of the Punjab, New Campus, Lahore 54590, Pakistan

Correspondence should be addressed to Zia ul-Haq; zia.spsc@yahoo.com

Received 18 February 2015; Revised 12 May 2015; Accepted 7 June 2015

Academic Editor: Pawan Gupta

The focus of this study is to assess spatiotemporal variability of tropospheric NO_2 over South Asia using data from spaceborne OMI during the past decade (2004–2015). We find an average value of NO_2 $1.0 \pm 0.05 \times 10^{15}$ molec/cm^2 and a significant decadal increase of 14%. The elevating NO_2 pollution over the region is linked to rise in motor vehicles and industrial and agricultural activities and increase in biomass fuel usage. The observed seasonality of NO_2 is associated with change in meteorological conditions and seasonal cycles of anthropogenic emissions. OMI data reveal a seasonal peak in spring followed by winter largely linked to metrological conditions and anthropogenic emissions from crop residue and biomass burning for heating purpose, and low concentration in summer is mostly attributed to meteorological conditions. Significant increase, up to 42%, in NO_2 concentrations over northwestern IGB, is observed connected to large scale postmonsoon crop residue events of 2010 and 2012. It is seen that NO_2 is mounting over all the hotspot locations and most of the cities. Dhaka shows the highest increase of 77% followed by Islamabad (69%), Kabul (68%), Korba (64%), Bardhaman (47%), and Lahore (40%). On the contrary, DG Khan has shown negative trend of –11%.

1. Introduction

Nitrogen dioxide (NO_2) plays an important role in the modification of radiative balance of the Earth's atmosphere by changing its oxidizing capacity and chemistry and by influencing the lifetimes of important greenhouse gases. Its high concentration in the troposphere adversely impacts inhabitants of the planet [1, 2]. NO_2 is mainly emitted during industrial burning, vehicle combustion, biomass fuel and crop residue burning, direct soil emissions, and natural lightning [3, 4]. The dominant sink of NO_2 is its oxidation process, involving hydroxyl radical (OH) and solar ultraviolet (UV) radiations, by which secondary pollutants such as ozone, nitric acid, methane, and aldehydes are produced [5–9].

Tropospheric NO_2 shows high spatiotemporal variability mainly modulated by local emission changes, seasonal cycles, and meteorological conditions. South Asia is experiencing severe air quality degradation due to high population growth rate, burgeoning urbanization and industrialization, expanding demand of agricultural products, and exponentially increasing energy consumption rate (e.g., [10–14]). Therefore, in order to develop the effective strategies to reduce its emissions, it is necessary to assess spatiotemporal distribution of NO_2 and identify its emission sources over the study region.

As far as tropospheric NO_2 assessments are concerned, no study has so far been carried out over the whole South Asian region. However, a few studies have been conducted only on some parts of South Asia to investigate spatiotemporal variations and to identify NO_2 emission hotspots using satellite remote sensing technique [15–20]. Recently, Ul-Haq et al. [20] assessed spatial and temporal patterns of NO_2 over Pakistan using Ozone Monitoring Instrument (OMI) retrieved data for the period 2004–2008. Renuka et al. [19] analyzed long-term changes of tropospheric NO_2 over south India using retrievals from GOME/ERS-2 and OMI/Aura during 1996–2014. They reported an increase in NO_2 column over Gadanki (13.48°N, 79.18°E). In spite of increase in anthropogenic emissions (e.g., population and vehicular traffic), these authors also found decreasing trend between eastern and western Ghats possibly linked with changes in land-use pattern limiting the soil emissions of NO_2. Ramachandran et al. [18] studied tropospheric NO_2 over India and identified NO_2 hotspots during 2002–2012 based

Figure 1: Geographical map of South Asia identifying locations of the NO_2 hotspots (*image source: Google Earth*).

on measurements from SCanning Imaging Absorption spectroMeter for Atmospheric CHartographY (SCIAMACHY, on board Envisat satellite; [21, 22]). The study of David and Nair [17] was based on OMI data to detect seasonal changes and trends over Indian region for a period from 2007 to 2008. Ten-year (1996–2006) data obtained from Global Ozone Monitoring Experiment (GOME) and SCIAMACHY were used to study trends and seasonality over India [15] and to detect and analyze global NO_2 hotspots [16].

However, compared to previous studies, the present study offers two advancements, that is, complete coverage of the South Asian region for the first time and usage of higher spatial resolution data from OMI to identify small and localized emission sources of NO_2. In this study, spatiotemporal distribution of tropospheric NO_2 and identification of hotspots in South Asia are presented by using OMI data for a period from October 2004 to January 2015.

2. Geography and Meteorology of South Asia

South Asia is the second most populous region in the world having population over 1667.8 million with land surface area of approximately 5,134,613 km^2. According to the South Asian Association for Regional Cooperation (SAARC), this region consists of eight countries: Afghanistan, Pakistan, India, Nepal, Maldives, Sri Lanka, Bangladesh, and Bhutan [23] (Figure 1).

The study region can be divided into five extensive physical subregions: the high Himalayan and Karakoram mountains in the north; the southern lowlands (Indus-Ganges-Brahmaputra) that expand from Pakistan to the delta lands of Bangladesh making up the core and densely populated areas; Balochistan Plateau, the most dry area of the study region that covers the Suleman and Kirthar mountains in southern boundary of Afghanistan and Pakistan; the peninsular India, dominated by the Deccan Plateau bordered by narrow and fertile coastal plains backed by elongated north-south mountain ranges called western Ghats and eastern Ghats; and the island realm that includes Sri Lanka and Maldives [24].

Monsoon weather systems are the dominant climatic factors for the most of South Asia especially in Pakistan and India. In winter season cold and dry winds flow outward due to a large high-pressure system over the Himalayas and down across South Asia causing small amount of rain, whereas, in spring, these winds diminish, resulting in hot and dry season. In June low pressure over landmass draws in clean, warm, and moist air from the Arabian Sea (ArS), Bay of Bengal (BoB), and Indian Ocean (InO). The uplifting and cooling of these moist monsoon winds result in heavy rain fall, but not all of South Asia receives substantial rainfall from the southwest monsoon. In much of Pakistan and the Indian state of Rajasthan, precipitation is low and variable, resulting in steppe and desert climates [25–28].

Eleven statistical significant hotspots of NO_2 concentration have been identified which include Delhi, Mumbai, Kolkata, Korba, Singrauli, Bardhaman, Pakur, and Angul located in India, Lahore and Karachi from Pakistan, and Dhaka sited in Bangladesh. The basic climatic parameters of these hotspots are shown in Figure 2.

3. Materials and Methods

3.1. NO_2 Retrievals by OMI/Aura. NASA's Aura satellite team, celebrating its 10th anniversary of operations, has provided vital data about the chemistry and dynamics of Earth's atmosphere from the surface through the mesosphere. This satellite carries four instruments, that is, High Resolution Dynamics Limb Sounder (HIRDLS), Tropospheric Emission Spectrometer (TES), Microwave Limb Sounder (MLS), and Ozone Monitoring Instrument (OMI). In this study, because of improved algorithms and sensitivity of OMI for NO_2 detection at lower atmosphere, we have used its tropospheric NO_2 daily averaged product (OMNO2d.003, level 3). This sensor is a wide-field-imaging grating spectrometer with horizontal resolution of $13 \times 24\,km^2$ at the nadir point and it uses push-broom mode to measure the backscattered solar radiations (270–500 nm with spectral resolution of about 0.5 nm, [29–31]). Tropospheric NO_2 columns are retrieved by using Differential Optical Absorption Spectroscopy (DOAS) analysis in the 405–465 nm spectral range [32, 33]. Details of data filtering, DOAS analysis and algorithm, and data quality control procedures can be found in NASA's online user's manual for OMI products (https://earthdata.nasa.gov/).

It has been well established that NO_2 measurements retrieved from satellites are in good agreement with *in situ* measurements and bottom-up emission inventories [34–40]. The studies of Boersma et al. [41] and Celarier et al. [42] reviewed and validated the OMI-NO_2 with ground (MAX-DOAS instruments) and aircraft (DC-8 aircraft) measurements. They showed a good agreement between the tropospheric OMI-NO_2 column and ground-based measurements,

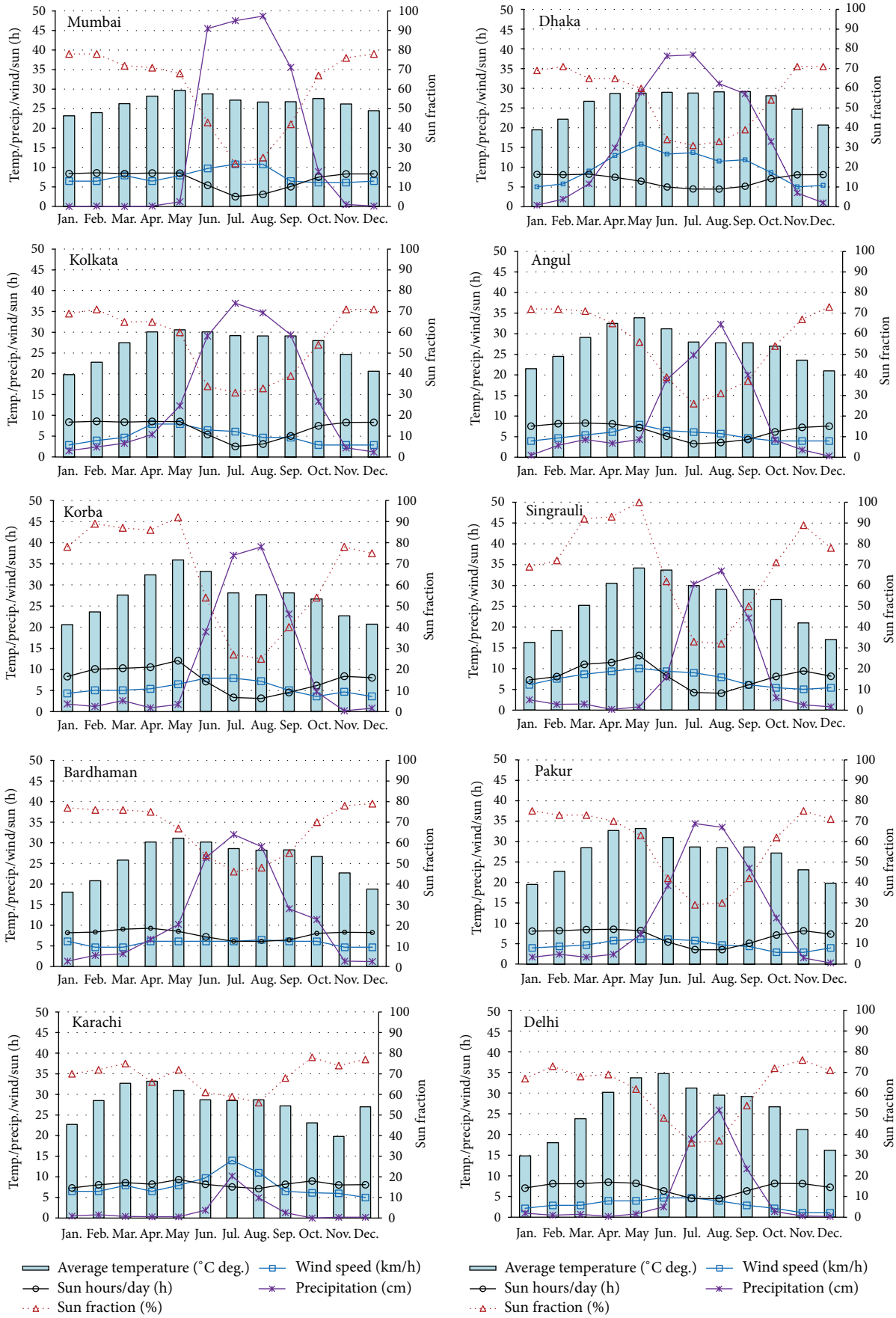

Figure 2: Continued.

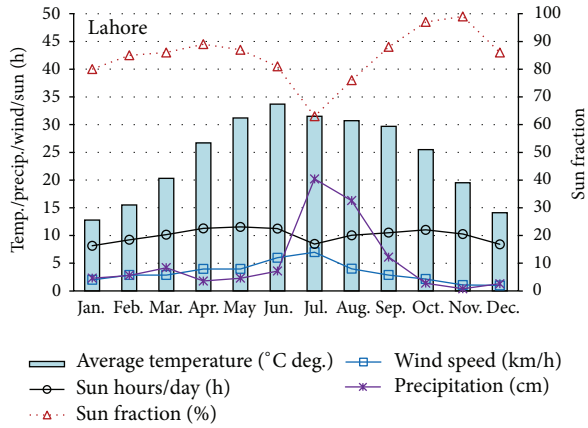

FIGURE 2: Climographs showing average temperature, sun fraction, precipitation, wind speed, and sun hours per day over NO_2 hotspots. Dotted line corresponds to secondary vertical axis.

with OMI-NO_2 columns underestimated by 15–30%. They also found a good correlation ($r = 0.83$) between the aircraft based NO_2 and OMI-NO_2 datasets. The observed OMI-NO_2 columns were smaller at about 15% (with uncertainty of ±10% and large scatter in the data) than the integrated *in situ* aircraft profiles. In a recent study, Ul-Haq et al. [20] found a good correlation ($r = 0.845$) between tropospheric OMI-NO_2 and SCIAMACHY-NO_2 columns using overpass data for the megacity Lahore (Pakistan).

3.2. Climate Data by Food and Agriculture Organization of United Nations (FAO). Monthly averaged climate data for NO_2 hotspots have been obtained from Food and Agriculture Organization of United Nations (FAO) global climate database using FAO Local Climate Estimator software New_LocClim, version 1.10 [43]. FAO has been using data from satellites and agrometeorological models [44, 45].

3.3. NO_2 Hotspots Identification. Higher values of a measurement may be very significant statistically but their spatial patterns are equally important if the data in hand is geographical in nature. In such a case spatial clustering of higher or lower values is of real importance to explain the phenomenon rather than the statistics of values only. In geostatistics, a feature will be significant if it has a high value and is surrounded by other features with high values as well. Geostatistical hotspot analysis compares proportionally local sum of NO_2 concentration for a feature and its defined neighborhood with sum of all the features in the study area.

In this study, geospatial statistic tool Getis-Ord G_i^* [46, 47] is used to identify statistically significant NO_2 concentration hotspots. The Getis-Ord G_i^* tool can be utilized for spatial clustering and autocorrelation [48]. This tool has been applied by using ArcGIS's Spatial Statistics tools and described in the following equations:

$$G_i^* = \frac{\sum_{j=1}^{n} w_{i,j}x_j - \overline{X}\sum_{j=1}^{n} w_{i,j}}{S\sqrt{\left[n\sum_{j=1}^{n} w^2{}_{i,j} - \left(\sum_{j=1}^{n} w_{i,j}\right)^2\right]/(n-1)}},$$

$$\overline{X} = \frac{\sum_{j=1}^{n} x_j}{n},$$

$$S = \sqrt{\frac{\sum_{j=1}^{n} x_j^2}{n} - \left(\overline{X}\right)^2}, \quad (1)$$

where x_j is the attributive value for a point j, $w_{i,j} = 1/r_{i,j}$ is distance of jth measurement point from ith measurement point, and n is the total number of measurement points (i.e., 23712 in this study). The calculated values of $\overline{X}$ are 0.724356 and 0.782528 for the years 2005–2008 and 2011–2014, respectively. Similarly, we find S values to be 0.665821 and 0.587949 for the data during 2005–2008 and 2011–2014, respectively. Getis-Ord G_i^* creates a new output feature class with z-score for each feature in the input feature class which indicates the place of a particular value in a dataset relative to the mean, standardized with respect to the standard deviation. The z-score represents the statistical significance (90% significant at $z \geq 1.645$, 95% significant at $z \geq 1.960$, 99% significant at $z \geq 2.576$, and 99.9% significant at $z \geq 3.291$) of clustering for a specified distance. For statistically significant positive z-scores, the larger the z-score, the more intense the clustering of high values (hotspot) [49]. A high z-score for a point indicates its neighbors have high attribute values and z-score near zero indicates that neighboring points have a range of values [50]. The Inverse Distance Squared Method, appropriate for this type of data where the closer features influence each other, with threshold distance of 1° has been used in hotspot identification [49]. We have obtained z-score values ranging from −4.43 to 22.18. Any location with its surrounding areas having sufficiently extreme z-score ($z \geq 10$) is selected to be a real statistically significant hotspot of NO_2 concentration.

In the present work, we have used annual mean values of OMI-NO_2 to calculate NO_2 average values, and the percentage increase calculation is based on linear trend line equation; that is, y-intercept represents initial concentration value. The correlations of hotspots are based on monthly mean values.

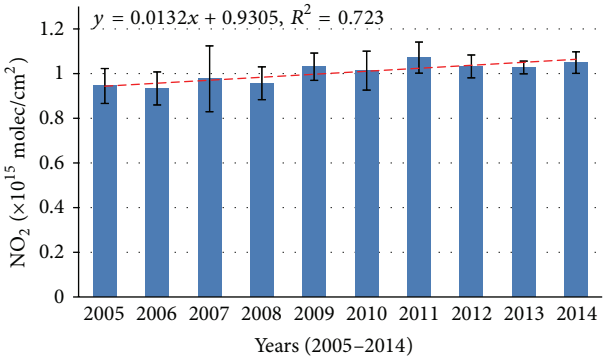

FIGURE 3: Area averaged annual distribution of OMI-NO_2 ($\times 10^{15}$ molec/cm^2) over the study region during 2005–2014.

4. Results and Discussion

4.1. Temporal Distribution of NO_2. The OMI retrievals show annual average value of tropospheric NO_2 column to be $1.0 \pm 0.05 \times 10^{15}$ molec/cm^2 over South Asia during the study period. A linear regression on the annual mean data shows a statistically significant (at confidence level of 99.9%) decadal increase of 14% with a slope of 0.013 (±0.002), correlation coefficient (R^2) 0.723, and y intercept at 0.930 (±0.017) $\times$ 10^{15} molec/cm^2. This positive trend is quite consistent with the trend (1.76 ± 1.1% per year) reported by Ghude et al. [16] for a region consisting of India, Pakistan, Bangladesh, and Nepal and trend reported by Ghude et al. [15] for India (1.67% per year). During the study period the highest annual value of 1.07×10^{15} molec/cm^2 is found in 2011 and lowest value of 0.93×10^{15} molec/cm^2 in 2006 (Figure 3).

The observed increase of NO_2 in the region may be attributed to increase in anthropogenic emissions due to expansion in traffic volume, increasing power generation, flourishing industries, rapid urbanization, more demand of agricultural products, and more biomass fuel usage (e.g., [10–16, 19, 20, 51–54]).

The main sources of NO_2 are different for South Asian countries. The level of urbanization in Pakistan is now the highest in South Asia [55]. During this period the escalating urban population, coupled with more demand in some sectors such as cement production, industrial expansion, motor vehicles usage, and electricity generation, has resulted in elevated levels of NO_2 emissions. In Pakistan road transport is the dominant mode of passengers that is responsible for carrying 91% of the national passenger traffic and 96% of the freight movements. During 2000 to 2010, the number of vehicles on the roads has grown from 4 to 9.8 million showing an increase of 145% [56]. The factors that are responsible for this huge increase are the import of reconditioned vehicles, popularity of vehicle financing schemes, and the President and the Prime Minister's Rozgar schemes (self-employment schemes) with heavy investments at low mark-up to purchase small auto vehicles like rickshaws and taxies [53]. The economy of Pakistan is heavily dependent on the agricultural sector. The total agricultural waste burnt is estimated to be 1704.9 thousand tons per year in the rice-wheat cropping system in Pakistan [57] contributing significant emissions of NO_2.

In India, the road transport is the dominant source of NO_2 emissions as compared to industry and power sector. The number of vehicles, registered in India, was 55 million in 2001 which has grown to around 159.5 million by 2012 [58]. Another important source of NO_2 emissions is the industrial process, especially the production of nitric acid, used in fertilizer manufacturing. India is an agrarian country and generates a large quantity of agricultural wastes. The annual crop residue generated in India for 2008-2009 is found to be about 620 Mt/year of which 15% is burnt on farms emitting huge amount of NO_x for the 2008-2009 [59]. Significant amount of NO_2 is emitted from coal fired power plants. India is the biggest energy user, followed by Iran and Pakistan. Coal is India's most abundant source of energy and currently almost 60% of its commercial energy needs are fulfilled by it. Lastly, widespread use of traditional sources of energy such as fuel wood and animal dung has also been contributing to NO_2 emissions. Estimates indicate that nearly 3 in 4 rural households depend on traditional sources of energy for cooking, heating, and so forth [60].

In Afghanistan, usage of electricity generators, biomass burning, and vehicular traffic are important sources of NO_2. The use of portable generators during power outages is a major source of NO_2 in the country. In Kabul alone, there are about 173,755 diesel and gasoline power generators in which 99.5% are used by households. Animal dung is also used in 85% of rural homes and in about 15% of urban homes for heating and cooking. The transport sector faces challenges of illegal import of used vehicles, continued use of very old and poorly maintained vehicles, poor quality of transport fuel, and limited road capacity leading to high emissions of air pollutants [61].

In Bangladesh, NO_2 is mainly emitted from energy transformation industries, motor vehicles, biomass burning for industrial processing and home cooking, burning of agricultural residues, and iron and steel industries. In Bhutan, the sector-wise emissions estimates of NO_2 indicate that domestic sources and vehicles are responsible for NO_2 emissions. As per Male Declaration-2000 [62], the sources of NO_2 in Sri Lanka include transport (46.8%), domestic use (37.1%), power generation (13.7%), industry (2.3%), and fuel conversion (0.1%). Bhutan is one of the few countries in the world where the environment is still protected largely due to its vast forest cover and widespread use of hydropower and biomass energy. Forest fires are the biggest sources of air pollution in Bhutan [63]. In Maldives, road traffic and domestic combustions are mostly responsible for NO_x air pollution. In Nepal, major NO_x sources are associated with the combustion of fossil fuels in industries, especially in the cement industry.

The estimated lifetime of NO_2 in the Planetary Boundary Layer (PBL) is 18–27 hours with considerable diurnal and seasonal variations [7, 64, 65]. However, in the middle and upper troposphere, NO_2 lifetime varies from several days to a week due to decreased OH and aerosol concentrations [6, 66, 67]. The NO_2 lifetime depends on meteorological conditions, its photolysis rate, surface emissions, length of day and night,

aerosols abundance, and OH and H_2O concentrations [18, 68, 69]. The meteorological conditions such as wind speed, temperature, humidity, and solar radiations flux affect NO_2 concentration via removal, transformation, and transport processes [68]. The hot and humid atmosphere enhances the removal of NO_2 through photolysis [18]. Also low wind speeds reduce NO_2 transport and its vertical air mixing thus elevating NO_2 concentration near emission sources [69].

OMI data show large seasonal amplitude with a monthly highest value of 1.58×10^{15} molec/cm^2 (in March 2011) and lowest value of 0.76×10^{15} molec/cm^2 (in July 2006). We also find high fluctuations in daily average values ranging from 2.01×10^{15} molec/cm^2 to 0.22×10^{15} molec/cm^2. The 10-year monthly mean (October 2004–January 2015) NO_2 behavior is presented in Figure 4.

The monthly pattern shows NO_2 maximum in spring season with a primary peak in March 1.22×10^{15} molec/cm^2 and secondary peak in May 1.13×10^{15} molec/cm^2. March peak is mainly attributed to low humidity, low wind speeds, and mild temperatures causing reduction in photolysis removal process of NO_2 hence stabilizing its concentration. Because of these factors, the NO_2 stability dominates the NO_2 removal through photolysis process of NO_2 due to the availability of more solar radiations in this month. In March, the lower concentration of OH (if the water vapor concentration is low enough) is considered a limiting factor of NO_2 photolysis to form HNO_3, the principal sink for NO_2 (e.g., [5]).

Relatively high values in March–May and October-November are also associated with emissions of NO_2 from large scale open field crop residue burning (nearly 7–10 tons of crop waste per hector) in the study area during wheat-rice rotation periods [12, 70–72]. In the study region, the main area for crop residue burning is IGB consisting of Lahore, Dera Ghazi Khan, Narowal, Hafizabad, and Faisalabad in Pakistan and states of Uttar Pradesh, Punjab, and Haryana in India [13, 53, 73].

A winter season high with a peak in December 1.07×10^{15} molec/cm^2, is due to meteorology (weak winds and dry weather conditions), heavy usage of biomass fuel for wintertime home heating especially in the northern areas, and less UV radiations available for the initialization of photolysis reactions that break down NO_2 [8, 20, 74, 75]. In winter, shallower boundary layer results in lower vertical dispersion which reduces the dilution and removal rates of NO_2. This may also contribute to NO_2 enhancement in wintertime [76].

Low NO_2 during wet summer, with a notable dip in August 0.80×10^{15} molec/cm^2, is linked to massive advection of moist clean air mass, increased actinic fluxes enhancing the photodissociation of NO_2, elevated levels of OH radical helping NO_2 removal from the atmosphere via HNO_3, and presumably less traffic activity due to reduced social and educational activities during very hot summer [16, 20, 77, 78]. During the rainy season, effect of lightning on the increase of NO_2 concentration is not clearly seen due to the opposing influence of rain washout discussed by Yoo et al. [78]. The washout of the SO_2 and NO_2 by rainfall has been a global and regional concern, since it plays an important role in

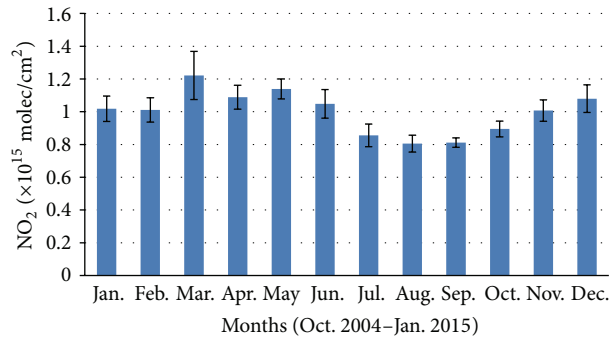

Figure 4: Area averaged monthly mean distribution of OMI-NO_2 ($\times 10^{15}$ molec/cm^2) over the study region during October 2004–January 2015.

producing acidic precipitation [78]. In the atmosphere, NO_2 reacts with water to form nitric or nitrous acid [79]. A number of previous studies have demonstrated significant negative correlation between NO_2 and rainfall (e.g., [77, 80, 81]). Martin [80] showed the washout coefficient for NO_2 is about 80% of that for SO_2. However, the washout effects on the NO_2 and SO_2 concentrations by daily cumulative rainfall are comparable over India, resulting in the reduction (40–45%) of these pollutants [77]. Yoo et al. [78] demonstrated the scavenging of air pollutants (CO, NO_2, SO_2, and PM_{10}) by summertime precipitation based on the three washout effect indicators such as Absolute Washout Index (AWI), Negative Correlation Fraction (NCF), and Relative Washout Index (RWI). They showed that the washout effect is in the descending magnitude order of $PM_{10} > SO_2 > NO_2 > CO > O_3$.

We discuss two crop residue burning events of postmonsoon 2010 [82] and postmonsoon 2012 [83]. South Asia is the principal niche of rice-wheat system that occupies a total of 13.5 million ha in rice-wheat consortium countries such as India, Pakistan, Bangladesh, and Nepal with rice cultivation areas of 10, 2.2, 0.8, and 0.5 million ha, respectively [57, 84]. In this regard, South Asian farmers need to manage 5–7 t ha^{-1} of rice residues and overcome the problems for planting wheat. There are various options for crop waste management out of which the burning of crop residue is one of the most common practices.

Elevated NO_2 concentrations have been found over northwestern parts of IGB including Punjab, Haryana, and western Uttar Pradesh regions as a direct consequence of the crop residue burning emissions (Figures 5(a)–5(c)). In Figure 4, NO_2 enhancements (10–42% on average) can be seen over the rice residue burning areas during the postmonsoon period of 2012, compared with the average value of postmonsoon periods during study years except 2010 and 2012, especially in Pakistani and Indian Punjab and their adjoining territories famous for rice cultivation. For the postmonsoon 2012, we find 15–35% increment in NO_2 levels showing close agreement with the results of Kaskaoutis et al. [83]. In a previous study, Kaskaoutis et al. [83] examined the impact of paddy crop residue burning over northern

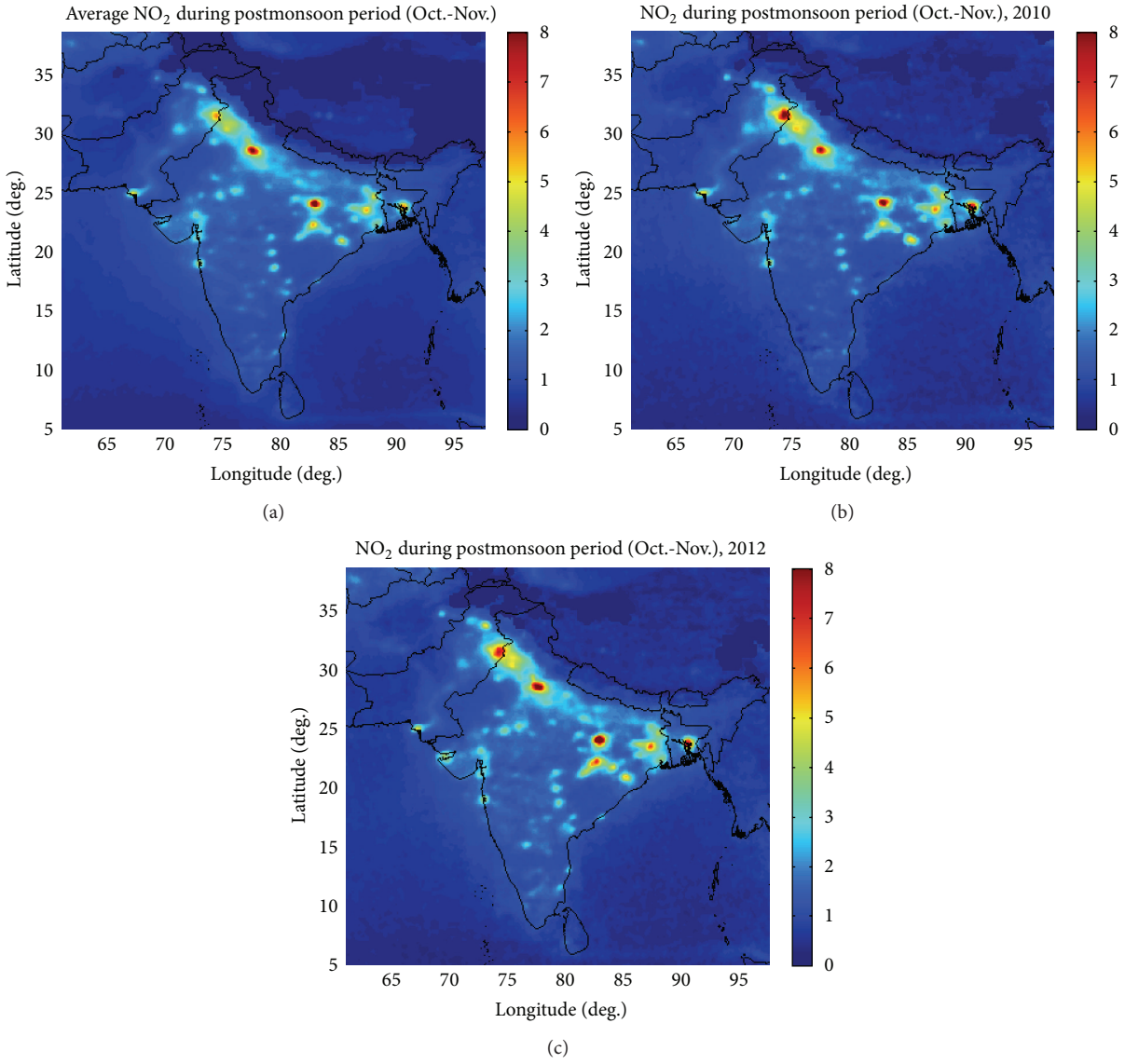

FIGURE 5: (a) Average NO_2 after monsoon for all years except 2010 and 2012. (b) NO_2 during postmonsoon 2010. (c) NO_2 during postmonsoon 2012.

India during the postmonsoon (October–November) season of 2012. They showed about 34–40% increase in NO_2 levels as a direct consequence of these crop residue burning events.

4.2. Spatial Distribution of NO_2. In Figure 6, an enhanced value of NO_2 observed over IGB is mainly coupled with high human settlement, coal based thermal power plants, industrialization and urbanization, more agricultural activity, large scale crop residue, and biomass mass burning previously reported by many studies (e.g., [3, 12, 19, 71, 85, 86]). It is evident from the figure that IGB section consisting of Punjab (from India and Pakistan) and eastern region of India show consistent high values due to high pupolation density, crop residue and biomass buning events, power plants, and mining activities. In addition, low population and rural areas scattered all over the region also contribute to NO_2 emissions from domestic cooking, small and medium industries, transport, and open burning of litter and biofuels. NO_2 masking is also observed over marine areas that is associated with NO_2 emissions due to seaport activities and urban pollution.

Our analysis shows significant decadal increasing trend of 17% (slope of 0.02428 ± 0.00657 and y intercept at $1.24751 \pm 0.03695 \times 10^{15}$ molec/cm^2) with average of $1.36 \pm 0.01 \times 10^{15}$ molec/cm^2 over a region between eastern and western Ghats (12.57–17.58°N to 76.05–79.00°E). This finding differs with the results by Renuka et al. [19] who reported a decreasing trend over the region between the two Ghats. The disparity in the results may be attributed to the difference in spatial and temporal domains.

4.3. NO_2 Hotspots in South Asia. In Figure 7(a), NO_2 hotspots have been identified and visualized during 2005–2014 using Getis-Ord G_i^* statistic hotspot analysis tool.

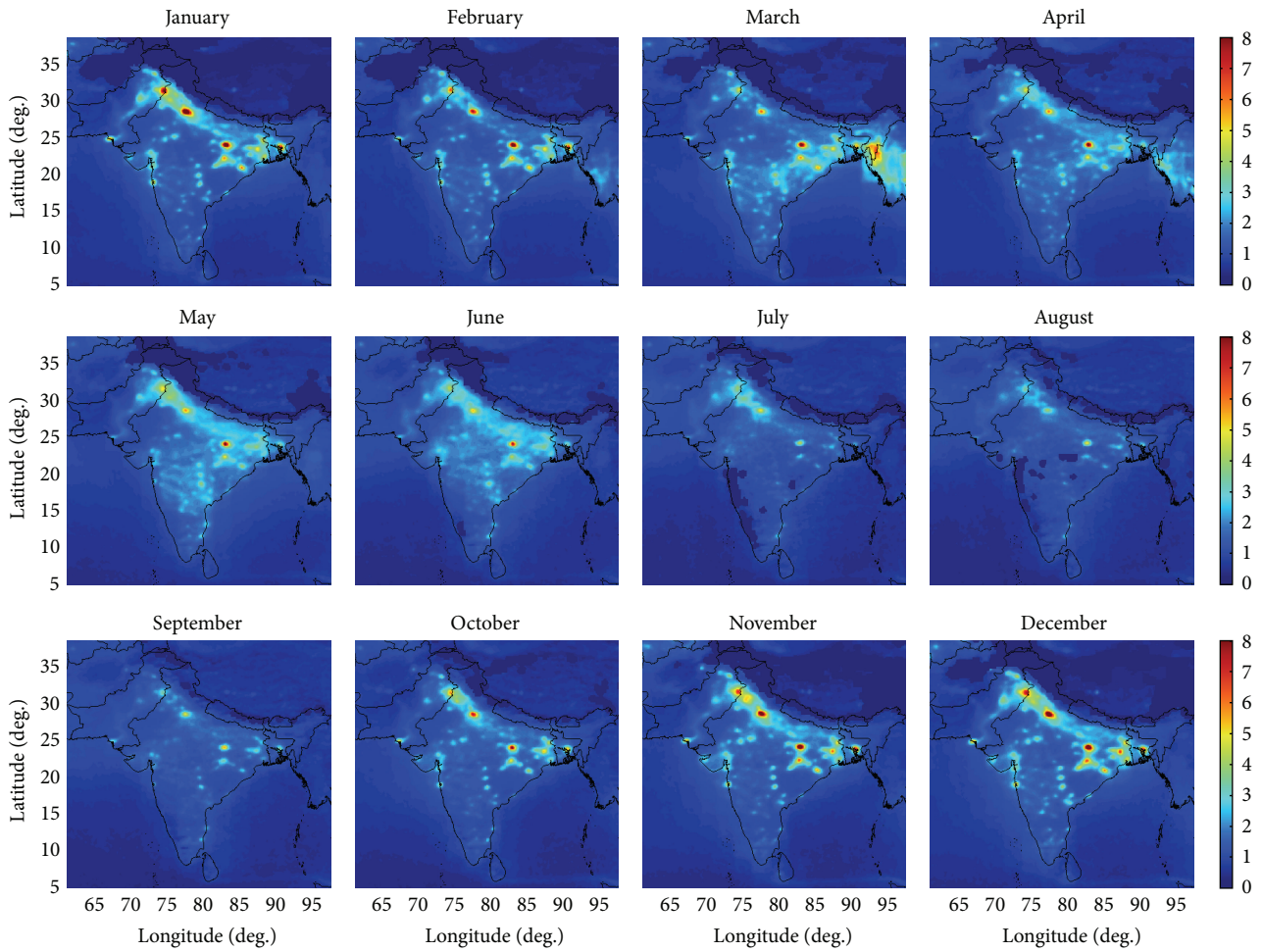

FIGURE 6: 10-year monthly mean spatial and temporal distribution of OMI/Aura tropospheric NO_2 ($\times 10^{15}$ molec/cm^2) over the study region during October 2004–January 2015.

These hotspots include megacities of Karachi and Mumbai located along the coastal belt of ArS, Lahore and Delhi sited in IGB, and Kolkata and Dhaka situated in eastern region of the study area.

It is evident from Figure 7(a) that high values of NO_2 are found over most of the hotspots observed in the northern areas. This NO_2 pollution appears more widespread over Lahore and Delhi as compared to other hotspots. This may be related to large scale crop residue burning and high population density in the surrounding territory. The lower NO_2 value over southern part of South Asia is due to a number of factors: small number of large point sources, low population density, less amount of biomass burning and vehicular population, and the hot and humid climate which leads to enhanced NO_2 photolysis.

In order to perform a more meaningful analysis of hotspots, we have created two time zones, namely, first four years (2005–2008) and last four years (2011–2014). The tendencies in the NO_2-hotspots are expressed in terms of differences in z-score values (Δz-score) and are calculated from the linear regression ($\Delta z\text{-score} = a * \Delta t$) to the time series for 2005–2008 and 2011–2014 periods individually. The averaged z-score values of the two periods are used to calculate the trends of hotspots. Δz-score actually represents the slope of the z-score regression line in each pixel starting in 01–01–2005 to 31–12–2008 (first period) and 01–01–2011 to 31–12–2014 (second period). From Figures 7(b)–7(d), it is revealed that negative trends of z-score cover some parts of IGB and central areas of India. The hotspots of Lahore, Delhi, Dhaka, Bardhaman, Pakur, and Korba are strengthening and expanding in geographical extent during both the periods. On the other hand, Mumbai, Karachi, Singrauli, Angul, and Kolkata are found to have decreasing trends. Cities of Islamabad, Kabul, and Ahmedabad also appear with significant increasing trends.

OMI data reveal that NO_2 columns are mounting over all the hotspots and most of the selected cities. However, the difference in increasing rates is mainly attributed to levels of the industrial activity, traffic volume, urban and rural background, and local meteorological conditions. Dhaka is the fastest growing city among all the hotspots and selected cities [87] linked to the highest increase (77%) in NO_2 column with an average of $3.15 \pm 0.51 \times 10^{15}$ molec/cm^2. After Dhaka, we find high growth rates for Islamabad 69%, Kabul 68%, Korba 64%, Bardhaman 47%, and Lahore 40%. On the other hand, DG Khan is found with negative trend at −11%.

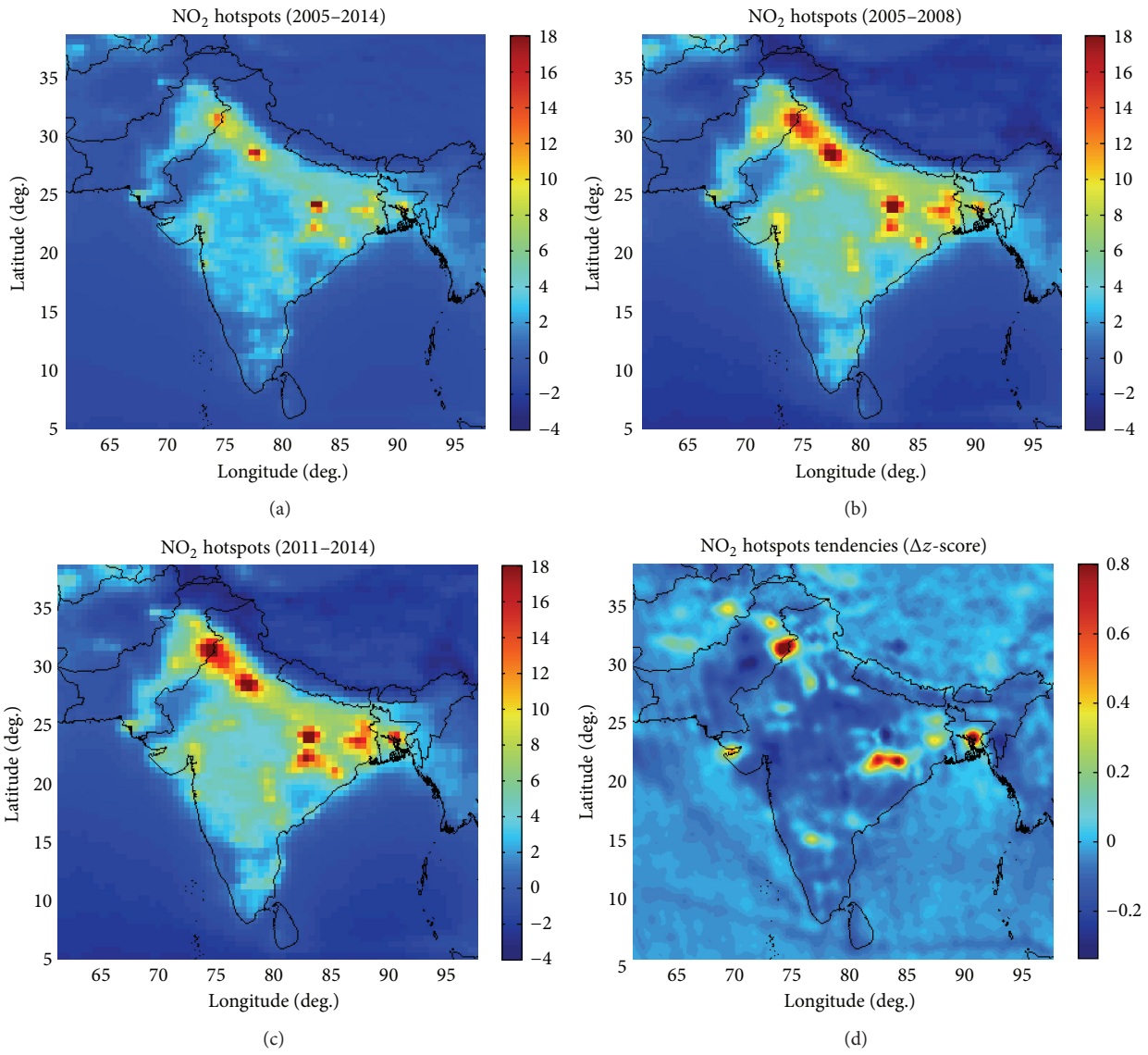

FIGURE 7: Spatial distribution of (a) hotspots during 2005–2014, (b) hotspots during 2005–2008, (c) hotspots during 2011–2014, and (d) hotspots tendencies (Δz-score) for 2005–2008 and 2011–2014.

The average value of NO_2 column over Singrauli is the highest $3.71 \pm 0.27 \times 10^{15}$ molec/cm^2 followed by Bardhaman $3.23 \pm 0.44 \times 10^{15}$ molec/cm^2 and Korba $3.23 \pm 0.44 \times 10^{15}$ molec/cm^2, whereas Karachi has exhibited the lowest average value of $2.00 \pm 0.10 \times 10^{15}$ molec/cm^2 with decadal increase at 6% (Table 1).

Figures 8 and 9 show the seasonality and intercomparison of the hotpots in the region. The megacities of Lahore and Delhi are located in IGB and experience almost the same meteorological conditions (Figure 2), large crop residue burning in surrounding areas, and extremity of monsoon which result in similarity in NO_2 seasonal patterns showing $R^2 = 0.865$ (Figures 7 and 8). Over Lahore and Delhi, higher NO_2 values are found during the winter months followed by spring season (Figure 6). Winter peak is mainly due to biomass burning for domestic heating [20], stable winds, less daily sun hours and sun fraction, and low temperature (Figure 2). In May, a surge in NO_2 over Lahore and Delhi is linked to large scale crop residue burning from wheat fields in the neighboring rural areas of Kasur, Shiekhupura, Narowal, Hafizabad, Mianchannu, and Uttar Pradesh regions. In this month, high temperature also contributes to soil emissions which are further enhanced by the application of fertilizers in the rice fields. The low NO_2 column over these cities during the period of monsoon season is mostly coupled with heavy rains, high humidity, and strong winds (Figure 2).

Some important anthropogenic emission sources of NO_2 in Lahore are industrial zones (e.g., Sundar industrial estate, Kot Lakhpat industrial area, Shahdara tractors manufacturing units, steel mills, and refrigerator manufacturing units), power plants (SEPCO, Kohinoor, Japan Power, and Nishat) and large scale crop residue burning events. Also a notable source of high NO_2, over Lahore, is the usage of diesel and petrol electricity generators during the heavy electric power

Table 1: Statistics of tropospheric NO_2 ($\times 10^{15}$ molec/cm^2) over South Asian countries, hotspots, and some major cities using OMI/Aura data during 2005–2014.

Name of the country/hotspot area/city	Location	Population (million)	Area (km^2)	Average ($\times 10^{15}$ molec/cm^2)	Decadal trend (%)	Trend parameters a = slope ± error b = y intercept ± error ($\times 10^{15}$ molec/cm^2)	Highest monthly value ($\times 10^{15}$ molec/cm^2)	Lowest monthly value ($\times 10^{15}$ molec/cm^2)
Bangladesh	23.70°N, 90.35°E	156.6	147,570	1.75 ± 0.13	23	$a = 0.04039 \pm 0.01063$, $b = 1.54966 \pm 0.05983$, $R^2 = 0.67337$	2.95 (Mar.-11)	0.95 (Jul.-05)
India	21.00°N, 78.00°E	1252	3,287,590	1.66 ± 0.08	17	$a = 0.02912 \pm 0.00452$, $b = 1.51498 \pm 0.02541$, $R^2 = 0.85592$	1.16 (Jul.-06)	2.36 (Mar.-11)
Afghanistan	34.53°N, 69.13°E	31	652,864	0.81 ± 0.04	16	$a = 0.01362 \pm 0.00358$, $b = 0.74361 \pm 0.02012$, $R^2 = 0.67459$	1.25 (Jul.-10)	0.49 (Oct.-05)
Nepal	26.53°N, 86.73°E	27	147,181	1.05 ± 0.05	13	$a = 0.01452 \pm 0.00464$, $b = 0.98200 \pm 0.02614$, $R^2 = 0.58262$	1.70 (Apr.-09)	0.71 (Jan.-06)
Pakistan	33.66°N, 73.16°E	182	796,095	1.24 ± 0.05	13	$a = 0.01706 \pm 0.00383$, $b = 1.15578 \pm 0.02154$, $R^2 = 0.73952$	1.53 (Jul.-10)	0.94 (Nov.-05)
Maldives	3.20°N, 73.22°E	0.3	300	0.20 ± 0.01	10	$a = 0.00239 \pm 0.00098$, $b = 0.19713 \pm 0.00549$, $R^2 = 0.46181$	0.33 (Feb.-06)	0.09 (Sep.-05)
Sri Lanka	7.00°N, 81.00°E	20.4	65,610	0.71 ± 0.01	6	$a = 0.00471 \pm 0.00203$, $b = 0.68708 \pm 0.01141$, $R^2 = 0.43601$	0.88 (May-06)	0.582 (Oct.-07)
Bhutan	27.41°N, 90.43°E	0.7	38,394	0.83 ± 0.04	5	$a = 0.00464 \pm 0.00628$, $b = 0.80861 \pm 0.03533$, $R^2 = 0.07251$	1.63 (Mar.-09)	0.48 (Aug.-05)
Dhaka (Dhaka Division, Bangladesh)	23.48°N, 90.24°E	14.39	815	3.15 ± 0.51	77	$a = 0.190 \pm 0.02121$, $b = 2.2012 \pm 0.119355$, $R^2 = 0.9198$	6.25 (Jan.-11)	1.31 (Jul.-06)
Islamabad (Capital of Pakistan)	33.40°N, 73.00°E	2.1	1060	2.32 ± 0.43	69	$a = 0.12912 \pm 0.03554$, $b = 1.67488 \pm 0.19997$, $R^2 = 0.65351$	4.68 (Dec.-10)	1.19 (Sep.-06)
Kabul (Capital of Afghanistan)	34.33°N, 69.08°E	3.5	425	1.74 ± 0.27	68	$a = 0.09677 \pm 0.01071$, $b = 1.26159 \pm 0.06026$, $R^2 = 0.92105$	5.03 (Jan.-13)	1.01 (Mar.-05)
Korba (Chhattisgarh, India)	22.35°N, 82.68°E	1.01	6,598	3.23 ± 0.44	64	$a = 0.1699 \pm 0.012827$, $b = 2.3838 \pm 0.072183$, $R^2 = 0.9616$	5.82 (Jun.-08)	1.44 (Feb.-05)

Table 1: Continued.

Name of the country/hotspot area/city	Location	Population (million)	Area (km^2)	Average ($\times 10^{15}$ molec/cm^2)	Decadal trend (%)	Trend parameters a = slope ± error b = y intercept ± error ($\times 10^{15}$ molec/cm^2)	Highest monthly value ($\times 10^{15}$ molec/cm^2)	Lowest monthly value ($\times 10^{15}$ molec/cm^2)
Bardhaman (West Bengal, India)	23.33°N, 87.30°E	0.34	56	3.23 ± 0.38	47	$a = 0.1363 \pm 0.011839$, $b = 2.5578 \pm 0.066623$, $R^2 = 0.9498$	5.89 (Dec.-13)	1.47 (Aug.-06)
Lahore (Punjab, Pakistan)	31.32°N, 74.22°E	10.23	1,172	3.22 ± 0.31	40	$a = 0.1176 \pm 0.013978$, $b = 2.6338 \pm 0.078661$, $R^2 = 0.91$	5.95 (Oct.-13)	1.82 (Sep.-06)
Pakur (Jharkhand, India)	23.30°N, 86.40°E	0.89	686	3.07 ± 0.26	35	$a = 0.102 \pm 0.008346$, $b = 2.5619 \pm 0.046963$, $R^2 = 0.9552$	5.19 (Sep.-12)	1.58 (May-05)
Chittagong (Chittagong Div, Bangladesh)	22.36°N, 91.80°E	*4.6*	157	1.61 ± 0.15	31	$a = 0.04878 \pm 0.01076$, $b = 1.37594 \pm 0.06054$, $R^2 = 0.74601$	4.03 (Mar.-11)	0.58 (Jul.-09)
Faisalabad (Punjab, Pakistan)	31.41°N, 73.07°E	6.5	5,856	2.48 ± 0.21	29	$a = 0.06997 \pm 0.01379$, $b = 2.13633 \pm 0.07759$, $R^2 = 0.78626$	3.79 (Jan.-11)	1.54 (Sep.-11)
Rajshahi (Rajshahi Division, Bangladesh)	24.36°N, 88.60°E	0.8	2,407	2.43 ± 0.19	26	$a = 0.06211 \pm 0.01320$, $b = 2.12518 \pm 0.07426$, $R^2 = 0.75987$	4.27 (Dec.-12)	1.16 (Jul.-10)
Bengaluru (Karnataka, India)	12.96°N, 77.56°E	4.30	741	1.88 ± 0.11	21	$a = 0.04048 \pm 0.00602$, $b = 1.67940 \pm 0.03390$, $R^2 = 0.86579$	3.33 (Mar.-11)	0.99 (Jul.-06)
Delhi (National Capital Region of India)	28.67°N, 77.22°E	16.31	1,484	3.20 ± 0.19	21	$a = 0.0697 \pm 0.008978$, $b = 2.8575 \pm 0.050523$, $R^2 = 0.896$	5.31 (Jan.-08)	1.99 (Aug.-06)
Singrauli (Madhya Pradesh, India)	24.12°N, 82.39°E	1.17	2,200	3.71 ± 0.27	21	$a = 0.0783 \pm 0.02638$, $b = 3.3193 \pm 0.148447$, $R^2 = 0.5574$	5.55 (Aug.-13)	1.55 (Aug.-11)
Angul (Odisha, India)	20.83°N, 85.01°E	1.27	6,232	2.73 ± 0.16	19	$a = 0.0527 \pm 0.013024$, $b = 2.4762 \pm 0.073292$, $R^2 = 0.7001$	4.59 (Mar.-11)	1.12 (Jul.-06)
Hyderabad (Telangana, India)	17.37°N, 78.48°E	9.5	650	2.06 ± 0.15	19	$a = 0.04071 \pm 0.01533$, $b = 1.86456 \pm 0.08629$, $R^2 = 0.50165$	3.6 (Mar.-11)	1.06 (Aug.-13)
Chennai (Tamil Nadu, India)	13.08°N, 80.27°E	4.34	426	2.33 ± 0.21	19	$a = 0.04669 \pm 0.02416$, $b = 2.10360 \pm 0.13594$, $R^2 = 0.34802$	3.31 (Mar.-11)	1.93 (Jul.-13)

Table 1: Continued.

Name of the country/hotspot area/city	Location	Population (million)	Area (km^2)	Average ($\times 10^{15}$ molec/cm^2)	Decadal trend (%)	Trend parameters a = slope ± error b = y intercept ± error ($\times 10^{15}$ molec/cm^2)	Highest monthly value ($\times 10^{15}$ molec/cm^2)	Lowest monthly value ($\times 10^{15}$ molec/cm^2)
Lucknow (Uttar Pradesh, India)	26.80°N, 80.90°E	3.7	2,528	2.14 ± 0.10	15	$a = 0.03362 \pm 0.00609$, $b = 1.97686 \pm 0.03427$, $R^2 = 0.81324$	2.99 (Jan.-12)	1.35 (Jul.-08)
Kolkata (West Bengal, India)	22.55°N, 88.31°E	14.11	1,886	2.63 ± 0.13	15	$a = 0.0411 \pm 0.011804$, $b = 2.4314 \pm 0.066426$, $R^2 = 0.6343$	4.27 (Oct.-10)	1.43 (Jul.-12)
Kathmandu (Capital of Nepal)	27.27°N, 85.33°E	0.7	50.67	1.03 ± 0.05	13	$a = 0.01412 \pm 0.00630$, $b = 0.96398 \pm 0.03546$, $R^2 = 0.41776$	1.85 (Apr.-09)	0.485 (Jan.-06)
Sylhet (Sylhet Division, Bangladesh)	24.90°N, 91.86°E	2.6	26.5	1.35 ± 0.01	12	$a = 0.01765 \pm 0.01109$, $b = 1.26824 \pm 0.06240$, $R^2 = 0.26568$	2.98 (Mar.-09)	0.61 (Jul.-05)
Gadanki (Andhra Pradesh, India)	13.48°N, 79.20°E	Few thousands	Few acres	1.16 ± 0.06	9	$a = 0.01194 \pm 0.00784$, $b = 1.10182 \pm 0.04410$, $R^2 = 0.24890$	2.16 (Mar.-11)	0.44 (Jul.-13)
Mumbai (Maharashtra, India)	19.04°N, 72.52°E	12.47	4,355	2.14 ± 0.08	7	$a = 0.0163 \pm 0.011462$, $b = 2.0635 \pm 0.064502$, $R^2 = 0.2243$	4.08 (Sep.-12)	0.48 (Aug.-09)
Karachi (Sindh, Pakistan)	24.51°N, 67.72°E	16.05	3,527	2.00 ± 0.10	6	$a = 0.0144 \pm 0.014674$, $b = 1.9283 \pm 0.082573$, $R^2 = 0.1211$	3.36 (Feb.-08)	1.08 (Sep.-11)
Ahmedabad (Gujarat, India)	23.03°N, 72.78°E	3.52	464	3.03 ± 0.10	4	$a = 0.01725 \pm 0.01369$, $b = 3.12073 \pm 0.07701$, $R^2 = 0.18491$	4.28 (Dec.-10)	1.727 (Jul.-05)
Colombo (Capital of Sri Lanka)	6.93°N, 79.84°E	6.4	37.31	1.32 ± 0.15	3	$a = 0.00503 \pm 0.02161$, $b = 1.30349 \pm 0.12158$, $R^2 = 0.00769$	3.3 (Jan.-12)	0.39 (Jul.-13)
Kanpur (Uttar Pradesh, India)	26.28°N, 80.24°E	2.5	1,680	2.17 ± 0.04	2	$a = 0.00442 \pm 0.00584$, $b = 2.15486 \pm 0.03285$, $R^2 = 0.07553$	2.99 (Dec.-13)	1.18 (Mar.-12)
DG Khan (Punjab, Pakistan)	30.03°N, 70.38°E	2.12	11,294	1.80 ± 0.12	−11	$a = -0.02401 \pm 0.01464$, $b = 1.92591 \pm 0.08238$, $R^2 = 0.27753$	2.53 (Jan.-08)	1.12 (Oct.-11)

FIGURE 8: Monthly mean values of OMI/Aura tropospheric NO_2 ($\times 10^{15}$ molec/cm^2) over the study area and hotspots during October 2004–January 2015.

load shedding (average 10–16 hours daily in city area) [53]. In Delhi, power plants (Badarpur, Rajghat, Pragati, and IPGCL), industrial estates (Badli, Wazirpur, Mangolpuri, Lawrance, Jhilmil Industrial Area, Patparganj, etc.), and biomass and crop residue burning are the notable contributors of NO_2 emissions. We find higher (17%) annual average value of tropospheric NO_2 $3.22 \pm 0.31 \times 10^{15}$ molec/cm^2 than the previously reported value $2.74 \pm 0.79 \times 10^{15}$ molec/cm^2 by Ul-Haq et al. [20] over Lahore for 2004–2008 using OMI data. The discrepancy between these two reported values is mainly due to the difference in time periods and increasing growth of anthropogenic emissions in the past few years.

The megacities of Karachi and Mumbai are considered as financial hubs of Pakistan and India, respectively. These cities are located in the coastal belt of ArS and show large similarity ($R^2 = 0.800$) in NO_2 column values, trends, and temporal variability (Table 1, Figure 9) mainly associated to matching meteorological and urban conditions. Karachi showed the lowest average value $2.00 \pm 0.10 \times 10^{15}$ molec/cm^2 with the lowest increase at 6% followed by Mumbai $2.14 \pm 0.08 \times 10^{15}$ molec/cm^2 with 7% increase during the study period. Ul-Haq et al. [20] reported higher $3.63 \pm 2.19 \times 10^{15}$ molec/cm^2 value of NO_2 over Karachi during 2004–2008 than our computed value. This decrease in NO_2 concentration over Karachi may be associated with the political instability and economic downturn in recent years. In Karachi and Mumbai, more than 80% of total NO_2 emissions come from industrial sector and fugitive emissions from oil and gas activities [18, 20]. It is clear from Figure 8 that high NO_2 occurs in winter over Karachi and Mumbai. These cities have poor conditions for NO_2 removal, transformation, and transport processes (low rainfall, low wind speed, and low ambient temperature) in winter months. Other contributing factor for high NO_2 may be NO_2 carrying wind (NW-NE) from Indian landmass areas amplified by local emissions. On the other hand, low values are observed in summer linked to more rain wash-out and high humidity and strong and clean sea breeze (Figure 2) from ArS. Major sectors of NO_2 emissions in Karachi are power plants (Bin Qasim I&II, Gul Ahmed, and Tapal), textile industry, steel and iron factories, chemical industry, oil refineries, and seaport activities. The core industrial area of major emissions in Mumbai and surrounding areas is the Mumbai-Pune belt that includes textiles, chemicals, engineering, electrical, drugs, transport equipment, plastic and synthetic goods, leather goods, and ship-building.

We find high correlation ($R^2 = 0.864$) between the NO_2 seasonality for Dhaka and Kolkata. NO_2 is found high over these cities throughout the dry season (October–March) and low for the rest of the year (April–September). Gurjar et al. [14] have reported that the ambient NO_2 level in Dhaka is 83 μg/m^3 which exceeds the World Health Organization (WHO) guideline concentration (40 μg/m^3). Annual 7–16%

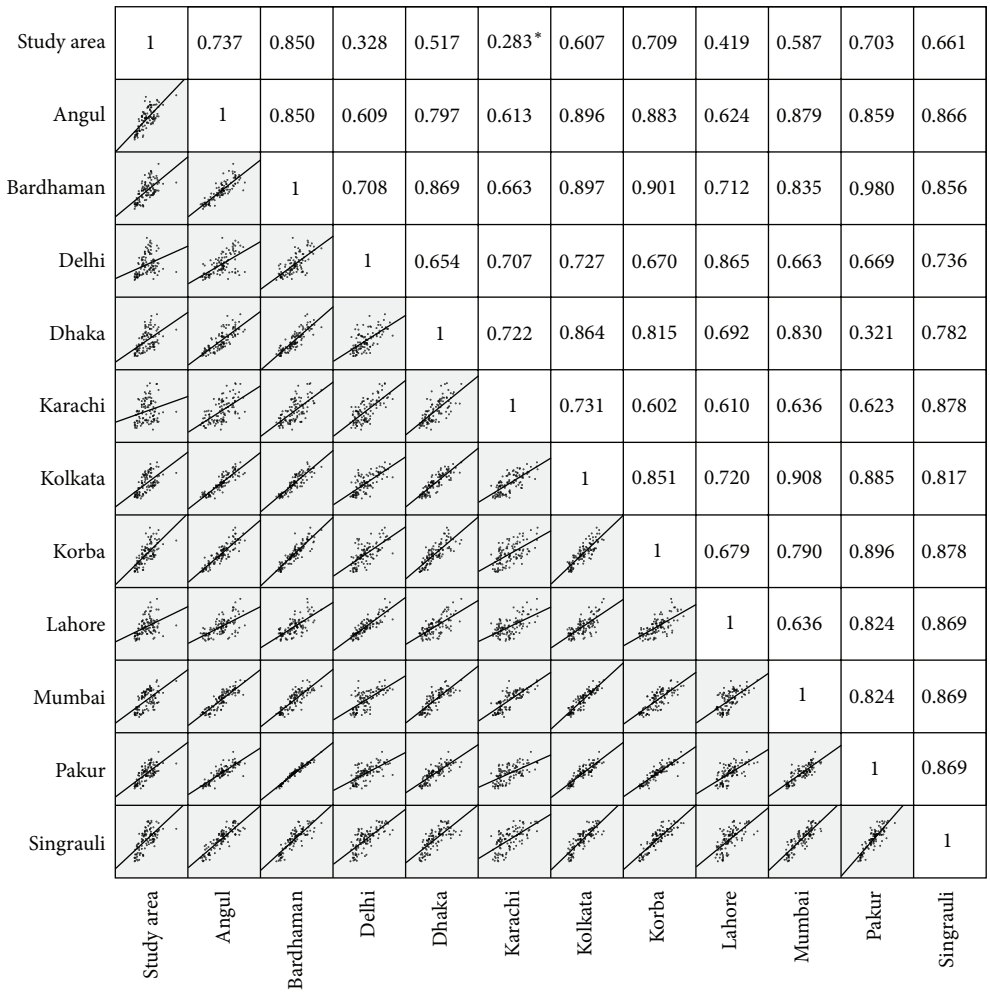

FIGURE 9: Correlation matrix of eleven NO_2 hotspots and study region with best fit curve. Pearson correlations values R^2 are also shown. All correlations are significant at the 0.01 level (2-tailed) except correlation between Karachi and the study area indicated by $*$ which is significant at the 0.05 level (2-tailed).

increase of vehicles has been observed for the last 10 years that has worsened the air quality as vehicular emissions are the single largest contributor of NO_2 in Dhaka [10, 88, 89]. The ambient NO_2 in Kolkata is observed to be 37 $\mu g/m^3$ [14] with the major emission sources of moderate to heavy vehicular traffic, power generation plants, rapid and unplanned urbanization and industrialization, and railway yard [11]. In Dhaka, a substantial part of total traffic is nonmotorized vehicles that produce severe congestion and pollution problem especially in road intersections. Other notable sectors which contribute to high NO_2 emissions are brick kilns, urban residential combustion, gas processing and refineries, and energy and manufacturing industries [90].

The highest correlation ($R^2 = 0.980$) is observed for Pakur and Bardharman and surrounding rural areas. These areas have very similar topography, low population, and meteorological conditions in agreement with Ramachandran et al. [18]. These hotspots have major sources of emissions as steel plants, major coal fields (Raniganj and Jharia), and crop residue burning in the adjoining territory. Singurali, Korba, and Angul hotspots are located in the eastern mining region (Singurali coalfield, Talchar coalfield, and Korba coalfields) of India [18]. Most of the mining processes and associated industries exist along with many of the major power plants and refineries in this region and cause high emissions and spread of NO_2 in this area [18, 85, 91, 92]. We have also found a similar seasonality ($R^2 = 0.908$) between NO_2 column over Mumbai and Kolkata as well, because both cities lie on almost similar latitude range and have tropical climate. Lower NO_2 values are observed over Mumbai compared to Kolkata primarily linked to strong winds (Table 1).

From Figure 7, it may be noted that there exists some difference between the NO_2 seasonality between the hotspots and South Asia. The NO_2 column over hotspots generally shows peak in December, while over South Asia it exhibits its elevated level in March. This is because of the fact that anthropogenic emissions dominate NO_2 seasonality over hotspots. On the other hand, March peak in South Asia, as a whole, is due to the dominance of natural factors discussed in Section 4.1.

5. Conclusions

OMI measurements over South Asia have been used to analyze spatial and temporal variability of tropospheric NO_2 column during October 2004 to January 2015. NO_2 emission hotspots and some important cities have been discussed for trends and seasonal cycles. An average value of $1.0 \pm 0.05 \times 10^{15}$ molec/cm^2 with 14% decadal increase has been reported over the study region. This positive trend is linked to the increasing anthropogenic emissions from power generation, urbanization, and vehicular and industrial sectors. Significant increase has been observed in NO_2 concentrations over some parts of IGB connected to large scale postmonsoon crop residue events of 2010 and 2012. Strong seasonality of NO_2 concentration is observed with the highest value in March and the lowest in August. Statistically significant NO_2 hotspots have been identified and discussed. OMI data reveal that the NO_2 columns are mounting at considerable rates over all the hotspot locations and most of the major cities. Dhaka (Bangladesh) showed the highest decadal increase, whereas Karachi (Pakistan) has exhibited the lowest average value of $2.00 \pm 0.10 \times 10^{15}$ molec/cm^2 with the lowest decadal increase at 6%. The highest average value is observed over Singrauli (India).

Conflict of Interests

The authors declare that there is no conflict of interests regarding the publication of this paper.

Acknowledgments

The authors thank three anonymous reviewers and the editor for improving the original paper. They greatly acknowledge NASA's team for OMI data (http://earthdata.com/) and FAO's team for New_LocClim, version 1.10.

References

[1] WHO, *Guidelines for Air Quality*, World Health Organization, Geneva, Switzerland, 2000.

[2] IPCC, "Climate change 2007: the physical science basis," in *Contribution of Working Group I to the Fourth Assessment Report of the Intergovernmental Panel on Climate Change*, S. Solomon, D. Qin, M. Manning et al., Eds., p. 996, Cambridge University Press, Cambridge, UK, 2007.

[3] A. Richter and J. P. Burrows, "Tropospheric NO_2 from GOME measurements," *Advances in Space Research*, vol. 29, no. 11, pp. 1673–1683, 2002.

[4] M. M. Cheng, H. Jiang, Z. Guo, and M. M. Cheng, "Evaluation of long-term tropospheric NO_2 columns and the effect of different ecosystem in Yangtze River Delta," *Procedia Environmental Sciences*, vol. 13, pp. 1045–1056, 2012.

[5] D. J. Jacob, *Introduction to Atmospheric Chemistry*, Princeton University Press, Princeton, NJ, USA, 1999.

[6] P. Warneck, *Chemistry of the Natural Atmosphere*, Academic Press, London, UK, 2000.

[7] T. Kunhikrishnan, M. G. Lawrence, R. Von Kuhlmann, A. Richter, A. Ladstätter-Weißenmayer, and J. P. Burrows, "Analysis of tropospheric NO_x over Asia using the model of atmospheric transport and chemistry (MATCH-MPIC) and GOME-satellite observations," *Atmospheric Environment*, vol. 38, no. 4, pp. 581–596, 2004.

[8] A. Richter, J. P. Burrows, H. Nüß, C. Granier, and U. Niemeier, "Increase in tropospheric nitrogen dioxide over China observed from space," *Nature*, vol. 437, no. 7055, pp. 129–132, 2005.

[9] Y. Kanaya, H. Tanimoto, J. Matsumoto et al., "Diurnal variations in H_2O_2, O_3, PAN, HNO_3 and aldehyde concentrations and NO/NO_2 ratios at Rishiri Island, Japan: potential influence from iodine chemistry," *Science of the Total Environment*, vol. 376, no. 1–3, pp. 185–197, 2007.

[10] A. K. Azad and T. Kitada, "Characteristics of the air pollution in the city of Dhaka, Bangladesh in winter," *Atmospheric Environment*, vol. 32, no. 11, pp. 1991–2005, 1998.

[11] M. K. Ghose, R. Paul, and S. K. Banerjee, "Assessment of the impacts of vehicular emissions on urban air quality and its management in Indian context: the case of Kolkata (Calcutta)," *Environmental Science and Policy*, vol. 7, no. 4, pp. 345–351, 2004.

[12] K. V. S. Badarinath, T. R. Kiran Chand, and V. Krishna Prasad, "Agriculture crop residue burning in the Indo-Gangetic Plains—a study using IRS-P6 AWiFS satellite data," *Current Science*, vol. 91, no. 8, pp. 1085–1089, 2006.

[13] K. V. S. Badarinath, S. K. Kharol, A. R. Sharma, and V. K. Prasad, "Analysis of aerosol and carbon monoxide characteristics over Arabian Sea during crop residue burning period in the Indo-Gangetic Plains using multi-satellite remote sensing datasets," *Journal of Atmospheric and Solar-Terrestrial Physics*, vol. 71, no. 12, pp. 1267–1276, 2009.

[14] B. R. Gurjar, T. M. Butler, M. G. Lawrence, and J. Lelieveld, "Evaluation of emissions and air quality in megacities," *Atmospheric Environment*, vol. 42, no. 7, pp. 1593–1606, 2008.

[15] S. D. Ghude, S. Fadnavis, G. Beig, S. D. Polade, and R. J. van der A, "Detection of surface emission hot spots, trends, and seasonal cycle from satellite-retrieved NO_2 over India," *Journal of Geophysical Research: Atmospheres*, vol. 113, no. 20, 2008.

[16] S. D. Ghude, R. J. Van der A, G. Beig, S. Fadnavis, and S. D. Polade, "Satellite derived trends in NO_2 over the major global hotspot regions during the past decade and their inter-comparison," *Environmental Pollution*, vol. 157, no. 6, pp. 1873–1878, 2009.

[17] L. M. David and P. R. Nair, "Tropospheric column O_3 and NO_2 over the Indian region observed by Ozone Monitoring Instrument (OMI): seasonal changes and long-term trends," *Atmospheric Environment*, vol. 65, pp. 25–39, 2013.

[18] A. Ramachandran, N. K. Jain, S. A. Sharma, and J. Pallipad, "Recent trends in tropospheric NO_2 over India observed by SCIAMACHY: identification of hot spots," *Atmospheric Pollution Research*, vol. 4, no. 4, pp. 354–361, 2013.

[19] K. Renuka, H. Gadhavi, A. Jayaraman, S. Lal, M. Naja, and S. V. B. Rao, "Study of ozone and NO_2 over Gadanki—a rural site in South India," *Journal of Atmospheric Chemistry*, vol. 71, no. 2, pp. 95–112, 2014.

[20] Z. Ul-Haq, S. Tariq, M. Ali, K. Mahmood, S. A. Batool, and A. D. Rana, "A study of tropospheric NO_2 variability over Pakistan using OMI data," *Atmospheric Pollution Research*, vol. 5, no. 4, pp. 709–720, 2014.

[21] J. P. Burrows, E. Hölzle, A. P. H. Goede, H. Visser, and W. Fricke, "SCIAMACHY—scanning imaging absorption spectrometer for atmospheric chartography," *Acta Astronautica*, vol. 35, no. 7, pp. 445–451, 1995.

[22] H. Bovensmann, J. P. Burrows, M. Buchwitz et al., "SCIAMACHY: mission objectives and measurement modes," *Journal of the Atmospheric Sciences*, vol. 56, no. 2, pp. 127–150, 1999.

[23] R. M. Joshi, "Education in South Asia," in *International Encyclopedia of the Social & Behavioral Sciences*, pp. 194–197, 2nd edition, 2015.

[24] UNEP, *United Nations Environment Programme and Development Alternatives (2008), South Asia Environment Outlook 2009: UNEP, SAARC and DA*, United Nations Environment Programme (UNEP), 2008.

[25] J. E. Schwartzberg, *A Historical Atlas of South Asia*, Oxford University Press, Oxford, UK, 1992.

[26] S. Bose and J. Ayesha, *Modern South Asia: History, Culture, and Political Economy*, Oxford University Press, Delhi, India, 2002.

[27] J. S. Bandara and Y. Cai, "The impact of climate change on food crop productivity, food prices and food security in South Asia," *Economic Analysis and Policy*, vol. 44, no. 4, pp. 451–465, 2014.

[28] R. Zhang, D. Jiang, Z. Zhang, and E. Yu, "The impact of regional uplift of the tibetan plateau on the asian monsoon climate," *Palaeogeography, Palaeoclimatology, Palaeoecology*, vol. 417, no. 1, pp. 137–150, 2015.

[29] P. F. Levelt, G. H. J. van den Oord, M. R. Dobber et al., "The ozone monitoring instrument," *IEEE Transactions on Geoscience and Remote Sensing*, vol. 44, no. 5, pp. 1093–1100, 2006.

[30] P. F. Levelt, E. Hilsenrath, G. W. Leppelmeier et al., "Science objectives of the ozone monitoring instrument," *IEEE Transactions on Geoscience and Remote Sensing*, vol. 44, no. 5, pp. 1199–1208, 2006.

[31] I. Zyrichidou, M. E. Koukouli, D. S. Balis et al., "Evaluation of high resolution simulated and OMI retrieved tropospheric NO_2 column densities over Southeastern Europe," *Atmospheric Research*, vol. 122, pp. 55–66, 2013.

[32] H. J. Eskes and K. F. Boersma, "Averaging kernels for DOAS total-column satellite retrievals," *Atmospheric Chemistry and Physics*, vol. 3, no. 5, pp. 1285–1291, 2003.

[33] J. Wallace and P. Kanaroglou, "The sensitivity of OMI-derived nitrogen dioxide to boundary layer temperature inversions," *Atmospheric Environment*, vol. 43, no. 22-23, pp. 3596–3604, 2009.

[34] K. F. Boersma, D. J. Jacob, M. Trainic et al., "Validation of urban NO_2 concentrations and their diurnal and seasonal variations observed from the SCIAMACHY and OMI sensors using in situ surface measurements in Israeli cities," *Atmospheric Chemistry and Physics*, vol. 9, no. 12, pp. 3867–3879, 2009.

[35] M. Hayn, S. Beirle, F. A. Hamprecht, U. Platt, B. H. Menze, and T. Wagner, "Analysing spatio-temporal patterns of the global NO_2-distribution retrieved from GOME satellite observations using a generalized additive model," *Atmospheric Chemistry and Physics*, vol. 9, no. 17, pp. 6459–6477, 2009.

[36] L. N. Lamsal, R. V. Martin, A. van Donkelaar et al., "Indirect validation of tropospheric nitrogen dioxide retrieved from the OMI satellite instrument: insight into the seasonal variation of nitrogen oxides at northern midlatitudes," *Journal of Geophysical Research: Atmospheres*, vol. 115, no. 5, Article ID D05302, 2010.

[37] V. Sheel, S. Lal, A. Richter, and J. P. Burrows, "Comparison of satellite observed tropospheric NO_2 over India with model simulations," *Atmospheric Environment*, vol. 44, no. 27, pp. 3314–3321, 2010.

[38] I. Kloog, F. Nordio, B. A. Coull, and J. Schwartz, "Incorporating local land use regression and satellite aerosol optical depth in a hybrid model of spatiotemporal PM2.5 exposures in the mid-atlantic states," *Environmental Science & Technology*, vol. 46, no. 21, pp. 11913–11921, 2012.

[39] G. Prud'homme, N. A. Dobbin, L. Sun et al., "Comparison of remote sensing and fixed-site monitoring approaches for examining air pollution and health in a national study population," *Atmospheric Environment*, vol. 80, pp. 161–171, 2013.

[40] A. Oluleye and E. C. Okogbue, "Analysis of temporal and spatial variability of total column ozone over West Africa using daily TOMS measurements," *Atmospheric Pollution Research*, vol. 4, no. 4, pp. 387–397, 2013.

[41] K. F. Boersma, D. J. Jacob, E. J. Bucsela et al., "Validation of OMI tropospheric NO_2 observations during INTEX-B and application to constrain NOx emissions over the eastern United States and Mexico," *Atmospheric Environment*, vol. 42, no. 19, pp. 4480–4497, 2008.

[42] E. A. Celarier, E. J. Brinksma, J. F. Gleason et al., "Validation of ozone monitoring instrument nitrogen dioxide columns," *Journal of Geophysical Research: Atmospheres*, vol. 113, no. 15, Article ID D15S15, 2008.

[43] FAO, *New_LocClim: Local Climate Estimator*, Environment and Natural Resources Working Paper No. 20, 2005, http://www.fao.org/nr/climpag/pub/en3_051002_en.asp.

[44] R. Gommes, F. L. Snijders, and J. Q. Rijks, *FAO Crop Forecasting Philosophy in National Food Warning Systems*, FAO, Rome, Italy, 1998.

[45] M. Bernardi and F. L. Snijders, "ARTEMIS software used by FAO for remotely sensed data," in *Proceedings of the World Meteorological Organization Expert Group Meeting on Software for Agroclimatic Data Management*, Washington, DC, USA, October 2000.

[46] A. Getis and J. K. Ord, "The analysis of spatial association by use of distance statistics," *Geographical Analysis*, vol. 24, no. 3, pp. 189–206, 1992.

[47] J. K. Ord and A. Getis, "Local spatial autocorrelation statistics: distributional issues and an application," *Geographical Analysis*, vol. 27, no. 4, pp. 286–306, 1995.

[48] T. Zhang, "Limiting distribution of the G statistics," *Statistics and Probability Letters*, vol. 78, no. 12, pp. 1656–1661, 2008.

[49] Esri, *ArcGIS Resources*, 2015, http://resources.arcgis.com/.

[50] A. Mitchell, *The Esri Guide to GIS Analysis*, vol. 2, ESRI Press, 2005.

[51] M. Ali, S. Tariq, K. Mahmood, A. Daud, A. Batool, and Zia-ul-Haq, "A study of aerosol properties over Lahore (Pakistan) by using AERONET data," *Asia-Pacific Journal of Atmospheric Sciences*, vol. 50, no. 2, pp. 153–162, 2014.

[52] Z. Ul-Haq, S. Tariq, A. D. Rana, M. Ali, K. Mahmood, and P. Shahid, "Satellite remote sensing of total ozone column (TOC) over Pakistan and neighbouring regions," *International Journal of Remote Sensing*, vol. 36, no. 4, 2015.

[53] Z. ul-Haq, A. D. Rana, M. Ali, K. Mahmood, S. Tariq, and Z. Qayyum, "Carbon monoxide (CO) emissions and its tropospheric variability over Pakistan using satellite-sensed data," *Advances in Space Research*, 2015.

[54] S. Tariq and M. Ali, "Spatio-temporal distribution of absorbing aerosols over Pakistan retrieved from OMI onboard aura satellite," *Atmospheric Pollution Research*, vol. 6, no. 2, pp. 254–266, 2015.

[55] Sustainable Development Policy Institute (SDPI), *Quarterly Pakistan Forest Digest, Vol. 01, No. 01*, Sustainable Development Policy Institute (SDPI), 2010.

[56] Pakistan Strategic Country Environmental Assessment, The World Bank, 2006, http://www.environment.gov.pk/new-pdf/PK-SCE-FText-Oct-2006%20.pdf.

[57] A. Tanvir and A. Bashir, "Why do farmers burn rice residue? Examining farmers' choices in Punjab, Pakistan. South Asian Network for Development and Environmental Economics (SANDEE)," Working Paper 76-13, 2013.

[58] RTYB, *Road Transport Year Book (2011-12), Transport Research Wing*, Ministry of Road Transport & Highways, Government of India, New Delhi, India, 2013.

[59] N. Jain, A. Bhatia, and H. Pathak, "Emission of air pollutants from crop residue burning in India," *Aerosol and Air Quality Research*, vol. 14, no. 1, pp. 422–430, 2014.

[60] MoE, *State of the Environment*, Ministry of Environment, Government of India, New Delhi, India, 2010, http://envfor.nic.in/soer/list.html.

[61] MoEP (Ministry of Economy and Planning), *Afghanistan Statistical Yearbook 2005*, 2005.

[62] Malé Declaration, Baseline Information and Action Plan, United Nations Environment Programme Regional Resource Centre for Asia and Pacific, 2000, http://www.rrcap.ait.asia/issues/air/maledec/baseline/indexsri.html.

[63] UNDP, United Nations Development Programme in Bhutan, 2015, http://www.bt.undp.org/content/bhutan/en/home/library/environment_energy/.

[64] C. Leue, M. Wenig, T. Wagner, O. Klimm, U. Platt, and B. Jähne, "Quantitative analysis of NO_x emissions from Global Ozone Monitoring Experiment satellite image sequences," *Journal of Geophysical Research: Atmospheres*, vol. 106, no. 6, pp. 5493–5505, 2001.

[65] D. Schaub, A. K. Weiss, J. W. Kaiser et al., "A transboundary transport episode of nitrogen dioxide as observed from GOME and its impact in the Alpine region," *Atmospheric Chemistry and Physics*, vol. 5, no. 1, pp. 23–37, 2005.

[66] L. Jaeglé, D. J. Jacob, Y. Wang et al., "Sources and chemistry of NOx in the upper troposphere over the United States," *Geophysical Research Letters*, vol. 25, no. 10, pp. 1705–1708, 1998.

[67] J. H. Seinfeld and S. N. Pandis, *Atmospheric Chemistry and Physics—From Air Pollution to Climate Change*, John Wiley & Sons, New York, NY, USA, 1998.

[68] P. S. Arya, *Air Pollution Meteorology and Dispersion*, Oxford University Press, New York, NY, USA, 1999.

[69] A. M. Jones, R. M. Harrison, and J. Baker, "The wind speed dependence of the concentrations of airborne particulate matter and NO_x," *Atmospheric Environment*, vol. 44, no. 13, pp. 1682–1690, 2010.

[70] S. Korontzi, J. McCarty, T. Loboda, S. Kumar, and C. Justice, "Global distribution of agricultural fires in croplands from 3 years of Moderate Resolution Imaging Spectroradiometer (MODIS) data," *Global Biogeochemical Cycles*, vol. 20, no. 2, 2006.

[71] A. K. Mishra and T. Shibata, "Synergistic analyses of optical and microphysical properties of agricultural crop residue burning aerosols over the Indo-Gangetic Basin (IGB)," *Atmospheric Environment*, vol. 57, pp. 205–218, 2012.

[72] H. S. Gadhavi, K. Renuka, V. Ravi Kiran et al., "Evaluation of black carbon emission inventories using a Lagrangian dispersion model—a case study over southern India," *Atmospheric Chemistry and Physics*, vol. 15, no. 3, pp. 1447–1461, 2015.

[73] C. Sarkar, V. Kumar, and V. Sinha, "Massive emissions of carcinogenic benzenoids from paddy residue burning in north India," *Current Science*, vol. 104, no. 12, pp. 1703–1709, 2013.

[74] I. H. Uno, Y. He, T. Ohara et al., "Systematic analysis of interannual and seasonal variations of model-simulated tropospheric NO_2 in Asia and comparison with GOME-satellite data," *Atmospheric Chemistry and Physics*, vol. 7, no. 6, pp. 1671–1681, 2007.

[75] T. Nishanth and K. M. K. Satheesh, "Increasing trends of tropospheric ozone and NO_2 at the prominent hot spots along the coastal belt of the Arabian Sea in Indian Subcontinent," *International Journal of Environmental Sciences*, vol. 1, no. 5, pp. 860–870, 2011.

[76] I. Barnes and K. J. Rudziński, Eds., *Disposal of Dangerous Chemicals in Urban Areas and Mega Cities: Role of Oxides and Acids of Nitrogen in Atmospheric Chemistry*, NATO Science for Peace and Security Series C: Environmental Security, Springer, Amsterdam, The Netherlands, 2013.

[77] K. Ravindra, S. Mor, A. Ameena, J. S. Kamyotra, and C. P. Kaushik, "Variation in spatial pattern of criteria air pollutants before and during initial rain of monsoon," *Environmental Monitoring and Assessment*, vol. 87, no. 2, pp. 145–153, 2003.

[78] J.-M. Yoo, Y.-R. Lee, D. Kim et al., "New indices for wet scavenging of air pollutants (O_3, CO, NO_2, SO_2, and PM_{10}) by summertime rain," *Atmospheric Environment*, vol. 82, pp. 226–237, 2014.

[79] S. Zumdahl and S. Zumdahl, *Chemistry*, Cengage Learning, 7th edition, 2006.

[80] A. Martin, "Estimated washout coefficients for sulphur dioxide, nitric oxide, nitrogen dioxide and ozone," *Atmospheric Environment*, vol. 18, no. 9, pp. 1955–1961, 1984.

[81] M. Q. Huo, Q. Sun, Y. H. Bai et al., "Chemical character of precipitation and related particles and trace gases in the North and South of China," *Journal of Atmospheric Chemistry*, vol. 67, no. 1, pp. 29–43, 2010.

[82] S. Tariq, Z. Ul-Haq, and M. Ali, "Analysis of optical and physical properties of aerosols during crop residue burning event of October 2010 over Lahore, Pakistan," *Atmospheric Pollution Research*. In press.

[83] D. G. Kaskaoutis, S. Kumar, D. Sharma et al., "Effects of crop residue burning on aerosol properties, plume characteristics, and long-range transport over northern India," *Journal of Geophysical Research: Atmospheres*, vol. 119, no. 9, pp. 5424–5444, 2014.

[84] K. G. Mandal, A. K. Misra, K. M. Hati, K. K. Bandyopadhyay, P. K. Ghosh, and M. Mohanty, "Rice residue-management options and effects on soil properties and crop productivity," *Journal of Food, Agriculture and Environment*, vol. 2, pp. 224–231, 2004.

[85] A. Garg, P. R. Shukla, S. Bhattacharya, and V. K. Dadhwal, "Sub-region (district) and sector level SO_2 and NO_x emissions for India: assessment of inventories and mitigation flexibility," *Atmospheric Environment*, vol. 35, no. 4, pp. 703–713, 2001.

[86] T. Kunhikrishnan, M. G. Lawrence, R. von Kuhlmann et al., "Regional NO_x emission strength for the Indian subcontinent and the impact of emissions from India and neighboring countries on regional O_3 chemistry," *Journal of Geophysical Research: Atmospheres*, vol. 111, no. 15, Article ID D15301, 2006.

[87] CMF, 2014. City Mayors Foundation, http://www.citymayors.com/statistics/urban_growth1.html.

[88] B. A. Begum, E. Kim, S. K. Biswas, and P. K. Hopke, "Investigation of sources of atmospheric aerosol at urban and semi-urban

areas in Bangladesh," *Atmospheric Environment*, vol. 38, no. 19, pp. 3025–3038, 2004.

[89] B. A. Begum, S. K. Biswas, and P. K. Hopke, "Assessment of trends and present ambient concentrations of $PM_{2.2}$ and PM_{10} in Dhaka, Bangladesh," *Air Quality, Atmosphere & Health*, vol. 1, no. 3, pp. 125–133, 2008.

[90] B. Sivertsen, S. Randall, S. Ahammad, and N. D. Cruz, *Modelled Concentrations of Criteria Air Pollutants in Dhaka and Chittagong PM_{10}, $PM_{2.5}$, NO_X, and SO_X for 2013 and 2020*, Norwegian Institute for Air Research (NILU), 2015.

[91] Z. Lu and D. G. Streets, "Increase in NOx emissions from indian thermal power plants during 1996–2010: Unit-based inventories and multisatellite observations," *Environmental Science & Technology*, vol. 46, no. 14, pp. 7463–7470, 2012.

[92] S. K. Sahu, G. Beig, and N. S. Parkhi, "Emerging pattern of anthropogenic NO_x emission over Indian subcontinent during 1990s and 2000s," *Atmospheric Pollution Research*, vol. 3, no. 3, pp. 262–269, 2012.